



# Optimization of Load Frequency Control parameters In hydro-wind systems using Manta Ray Foraging Optimization

Gabriel Schreider da Silva<sup>1</sup>, Lucas Santiago Nepomuceno<sup>1</sup>, Edimar José de Oliveira<sup>1</sup>, Arthur Neves de Paula<sup>1</sup>, Leonardo Willer de Oliveira<sup>1</sup>, Ivo Chaves da Silva Júnior<sup>1</sup>

<sup>1</sup>*Dept. of Energy, Federal University of Juiz de Fora  
Minas Gerais, Brazil*

*gabriel.schreider2016@engenharia.ufjf.br, lucas.nepomuceno@engenharia.ufjf.br,  
edimar.joliveira@engenharia.ufjf.br, arthur.paula@engenharia.ufjf.br,  
leonardo.willer@ufjf.edu.br, ivo.junior@ufjf.br*

## Abstract.

This work proposes a novel hybrid optimization approach combining nonlinear programming and the Manta Ray Foraging Optimization (MRFO) metaheuristic to optimize the controller parameters of the hydro-wind interconnected power system to improve the Load Frequency Control (LFC). The optimization process addresses challenges posed by integrating wind power into power grids due to its limited inertia, which hampers natural inertial response. The research focuses on incorporating wind generation into Load Frequency Control (LFC) utilizing the Virtual Synchronous Generator (VSG) technique and operational adjustments. In this way, this work contributes to improving LFC efficiency in mixed power generation setups by introducing a hybrid method that surpasses the limitations of traditional controllers, enhancing the equilibrium between power generation and demand.

**Keywords:** Manta Ray Foraging Optimization, nonlinear programming, Load Frequency Control, Wind generation, Hydro generation

## 1 Introduction

The rapid global growth of wind generation is evident, with installed capacity reaching 828.4 GW in 2021 from 220 GW in 2011, signifying a remarkable 376.55% increase in a decade [1]. Brazil experienced wind capacity growth by 1227.56%, from 2057 MW in April 2013 to 25251 MW in April 2023, positioning wind power as the second-largest source at 13.7% compared to hydroelectric generation's dominant 59.3% [2]. This prompts the need for enhanced studies to address operational challenges in hydro-wind power systems.

The integration of wind turbines impacts system inertia due to their disconnection from grid frequency. Consequently, they cannot offer inertial response during grid disturbances, potentially leading to frequency instability. Additionally, wind turbines' Maximum Power Point operation lacks reserve capacity, hindering their inclusion in Load Frequency Control [3]. Hydraulic turbines face the inverse response problem, further complicating the intricate task of designing effective Load Frequency Control for hydro-wind systems [4, 5].

In [3], the authors propose the incorporation of virtual inertia from wind generation into the LFC and the damping of oscillations in interconnection lines in hydro-wind power systems. The optimization approach proposed involves tuning both hydro and VSG (Virtual Synchronous Generator) controllers and is based on the time-response domain. The optimization problem is solved using the MATLAB optimization package based on the interior point method called *fmincon* [6].

Metaheuristic optimization leverages nature-inspired intelligent behaviors to tackle intricate challenges and enhance traditional optimization methods. By deftly balancing exploration and exploitation through stochastic operators spanning the search space, metaheuristics navigate complex problems efficiently, albeit at the risk of slower convergence when prioritizing exploration. A example is the Manta Ray Foraging Optimization (MRFO) algorithm, inspired by manta rays' astute foraging behaviors. This swarm-based approach incorporates three distinct foraging strategies—chain, cyclone, and somersault—mirroring manta rays' search patterns and offering a

robust framework for diverse optimization tasks, marking a significant advancement in optimization methodologies [7, 8].

Recent research has focused on exploring the applicability of the MRFO algorithm, particularly in power system optimization. One instance is the MRFO algorithm introduced in [9], which employs mathematical spiral foraging strategies to solve Economic Load Dispatch (ELD) problems with transmission losses. By utilizing various mathematical spirals, the algorithm enhances global search capabilities and convergence rates, demonstrating superiority over benchmark functions. A similar approach is seen in [10], where the MRFO algorithm optimizes Support Vector Regression (SVR) for short-term electrical load forecasting, achieving high precision in real data experiments. In [11], the MRFO algorithm is applied to Load Frequency Control (LFC) in interconnected power systems, showcasing its efficacy in optimizing proportional-integral-derivative (PID) controllers, supported by simulations with real-site data. Additionally, [12] presents the Multi-Strategy Improved Adaptive Manta Ray Foraging Optimization (MSAMRFO) algorithm for computing renewable energy hosting capacity in distribution networks, outperforming the original MRFO algorithm in terms of convergence speed and stability. This paper proposes a hybrid method that combines nonlinear programming with the MRFO algorithm to optimize Load Frequency Control (LFC) parameters in complex power systems, providing a promising avenue for surpassing the limitations of traditional control techniques and nonlinear optimization.

Under this background, this work introduces a hybrid method merging nonlinear programming and the Manta Ray Foraging Optimization (MRFO) metaheuristic to optimize Load Frequency Control (LFC) parameters in a two-area hydro-wind power system. LFC's significance lies in synchronizing power generation and demand while minimizing losses. Existing control techniques like adaptive controllers and sliding mode control (SMC) are effective but burdened by complexity, expertise-dependent parameter tuning, and elevated costs. Traditional controllers are simpler but struggle with non-linearities and sensitivity to parameter changes. The proposed metaheuristics risk local minima traps and complex tuning. The hybrid methodology presented offers a promising solution for LFC optimization in complex power systems. This hybridization technique enables an efficient search for solutions that surpass the inherent limitations of nonlinear optimization, thereby leading to the discovery of enhanced solutions.

## 2 Methodology

The proposed optimization strategy employs a time-response framework, enabling simultaneous tuning of all optimization variables. This approach aims to improve both the system's time response and dynamic damping in a unified manner. For hydro power plants, the methodology harmonizes the tuning of PID controllers and Transient Droop Compensators (TDC) as well as integral controller and Wind Power Dispatch Control (WPDC) of VSG is introduced. While VSG has been commonly used to enhance system inertia due to its fast response, this study explores an additional capability of VSG to reduce oscillations in interconnected hydro systems. By leveraging the converter's rapid response, VSG can dampen persistent oscillations in interconnection transmission lines, alongside its frequency control function.

The proposed search process comprises two distinct stages: Stage-1 involves Nonlinear Optimization using the Interior Point Method, and Stage-2 entails Refinement using the Meta-Heuristic MRFO.

To easy understand the explanation of the proposed methodology, the Figure (1) shows the system to be optimized. For each hydro plant, the variables that should be optimized are:  $K_p$ ,  $K_i$ ,  $K_d$ ,  $T_d$ ,  $R_t$ ,  $T_R$ ,  $B$  and  $g$  named respectively as follow: proportional, integral, derivative gains and the time constant of the derivative filter of the PID controller, temporary droop parameter, the reset time, Bias and tie line gain. The other hydro parameter are:  $T_G$  is the hydro turbine speed governor time constant;  $T_W$  is the water starting time;  $\Delta P_{L,h}$  is the active power load perturbation;  $K_{12}$  is the transmission line constant,  $\Delta P_{12}$  is the tie line power deviation,  $\Delta P_G$  is the active power generation deviation;  $\Delta GV$  is the valve speed of the governor;  $K_{ps}$  is the power system gain,  $T_{ps}$  is the power system time constant;  $\Delta FR$  is the frequency variation,  $R_p$  is the permanent governor speed regulation parameter;  $\frac{1}{R}$  is the droop characteristic;  $\dot{X}_{GV}^{close}$  is the valve opening speed limit (maximum valve speed);  $\dot{X}_{GV}^{open}$  is the valve closing speed limit (minimum valve speed);  $X_{GV}^{close}$  is the valve opening limit (maximum valve position) and  $X_{GV}^{open}$  is the valve closing limit (minimum valve position). On the other hand, the optimization variables of VSG are: the integral gain of the GSV controller,  $K_{i,v}$  and integral gain of the wind power dispatch control,  $K_{dc,v}$ . Finally, the constants variables are: the time constant of the wind power dispatch control,  $T_{dc,v}$  and the time constant of the virtual mechanical actuator,  $T_v$ . Therefore, this system has eighteen variable to be optimized.

### 2.1 Stage 1: Nonlinear Optimization

The initial focus is on solving the optimization problem using nonlinear techniques based on the Interior Point Method. The objective function is the integral of time squared error (ITSE), a metric previously utilized in

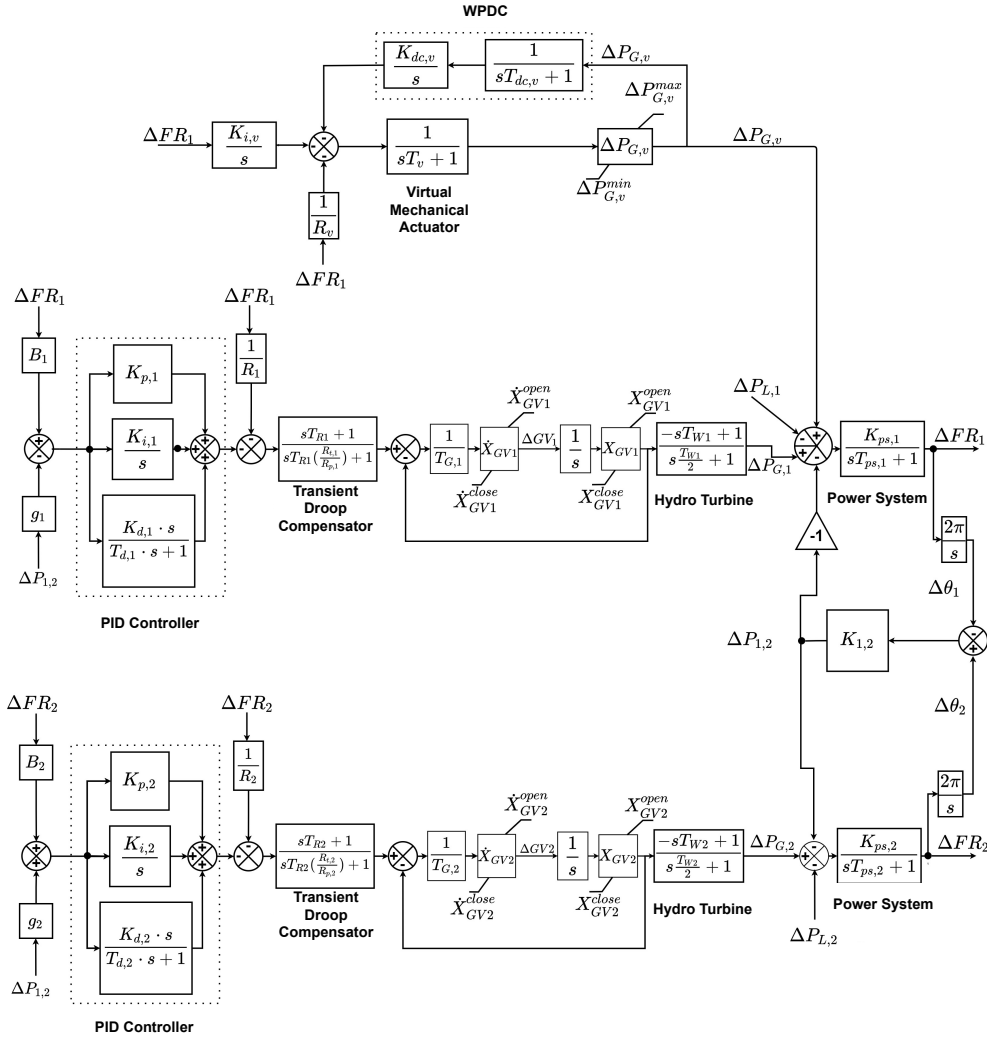


Figure 1. Hydro-Wind power system.

studies concerning Load Frequency Control (LFC) investigations [13]. The principal objective revolves around minimizing the squared deviation from the system's established equilibrium point. To ensure realistic outcomes, constraints are introduced to limit the optimization variables. The optimization problem is described as follow:

$$\begin{aligned}
 \text{Min } 10^6 \cdot & \left[ 5 \cdot \left( \sum_{t=1}^{t_{end}} \Delta f_1(t)^2 + \sum_{t=1}^{t_{end}} \rho^u \cdot (\Delta z_1(t) - z_{sat,1}^u)^2 + \sum_{t=1}^{t_{end}} \rho^d \cdot (\Delta z_1(t) - z_{sat,1}^d)^2 \right) \right. \\
 & + 5 \cdot \left( \sum_{t=1}^{t_{end}} \Delta f_2(t)^2 + \sum_{t=1}^{t_{end}} \rho^u \cdot (\Delta z_2(t) - z_{sat,2}^u)^2 + \sum_{t=1}^{t_{end}} \rho^d \cdot (\Delta z_2(t) - z_{sat,2}^d)^2 \right) \\
 & \left. + \left( \sum_{t=1}^{t_{end}} \Delta P_{1,2}(t)^2 \right) \right] \quad (1)
 \end{aligned}$$

Subject to:

$$X_i^{S1,min} < X_i^{S1} < X_i^{S1,max} \quad (i = 1, \dots, N_{val}). \quad (2)$$

where  $t$  indicates the specific time instant;  $\Delta f_1(t)$  and  $\Delta f_2(t)$  denote the time-dependent output frequency deviations in Area 1 and Area 2, respectively. Similarly,  $\Delta z_1(t)$  and  $\Delta z_2(t)$  represent the time-dependent output deviations considering the limiter effect, encompassing the limit deviations of power generation, valve speed, and

position for Area 1 and Area 2. The values  $z_{sat,1}^u$  and  $z_{sat,2}^u$  stand for the upper saturation thresholds for the variables  $\Delta z_1(t)$  and  $\Delta z_2(t)$ , respectively, while  $z_{sat,1}^d$  and  $z_{sat,2}^d$  represent the lower saturation thresholds. Furthermore, the symbols  $\rho^u$  and  $\rho^d$  serve as penalization parameters ensuring the satisfaction of saturation constraints for all instances of  $t$ . Specifically, these parameters are set to zero if  $\Delta z_1(t)$  and  $\Delta z_2(t)$  remain within their respective saturation limits ( $y_{sat}^u$  and  $y_{sat}^d$ ). Conversely, if the deviations exceed these limits at any time point, either  $\rho^u$  or  $\rho^d$  takes a value of 1000, effectively penalizing violations. The high penalization value aims to enforce a suitable temporal response while preventing limit breaches. Moreover,  $X_i^{S1}$  represents the  $i$ -th variable subject to optimization in Stage 1, with  $X_i^{S1,min}$  and  $X_i^{S1,max}$  denoting its lower and upper bounds. Additionally,  $t_{end}$  signifies the final simulation time, and  $N_{val}$  corresponds to the count of optimization variables under consideration.

## 2.2 Stage 2: Refinement using Meta-Heuristic MRFO

Following the completion of the first stage, the obtained solution may not be the global optimum. Therefore, the proposed methodology incorporates the use of the MRFO meta-heuristic [7] to conduct a search around the solution obtained in the Stage-1. In other words, MRFO can be described as a process of exploration around the Stage-1 solution. This stage comprises three main procedures:

- **Establishment of Search Bounds:** The determination of search boundaries involves setting upper and lower limits within the search space, expressed as a percentage deviation from the Stage-1 solution. The search space is bounded according to equations (3) - (5).
- **Generation of Initial Population:** The Initial Population is composed of  $N_{ind}$  individuals. This population includes  $N_{ind} - 1$  individuals that are randomly generated within the new boundaries, in addition to the solution  $X^{S1}$  acquired during the Stage-1.
- **MRFO Optimization Process:** Once the initial population of  $N_{ind}$  individuals is formed, the evolutionary journey of the meta-heuristic MRFO begins. This process advances until the predefined maximum number of iterations is attained. The MRFO strategy draws inspiration from the diverse foraging behaviors of manta rays as they seek sustenance in the oceans. The algorithm integrates three operators influenced by various foraging behaviors, including chain foraging, cyclone foraging, and somersault foraging [7]. The fitness value of each individual is calculated utilizing equation (1). Figure 2 depicts a simplified flowchart of the methodology proposed in this work.

$$X_i^{S2,max} = \min \left( X_i^{S1} \cdot (1 + \phi), X_i^{S1,max} \right). \quad (3)$$

$$X_i^{S2,min} = \max \left( X_i^{S1} \cdot (1 - \phi), X_i^{S1,min} \right). \quad (4)$$

$$X_i^{S2,min} < X_i^{S2} < X_i^{S2,max} (i = 1, \dots, N_{val}). \quad (5)$$

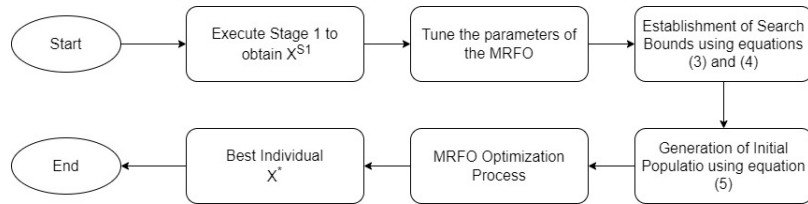


Figure 2. Flowchart of Hybrid Methodology.

where  $X^{S1}$  stands for the reference vector derived from Stage 1's solution.  $X_i^{S2,max}$  and  $X_i^{S2,min}$  represent the upper and lower limits respectively for optimization variable  $i$  in the second stage of our proposed methodology. The parameter  $\phi$  is the user-defined percentage factor, determining the proportion of the Stage-1 reference solution that shapes the boundaries of the search space in Stage-2.

## 3 Simulations and Results

The system diagram displayed in Figure (1) is used to show the effectiveness of the proposed approach and the system data can be found in <https://github.com/gopt-ufjf>. Four cases are considered as follows:

- Case 1: Only the *Stage-1* method is used to tune all the parameters.

- Case 2: The proposed hybrid method is employed, considering a search space of 10% around the the solution obtained in Case 1.
- Case 3: The proposed hybrid method is employed, considering a search space of 25% around the solution obtained in Case 1.
- Case 4: The proposed hybrid method is employed, considering a search space of 50% around the solution obtained in Case 1.

The simulations were conducted using a PC with an Intel Core *i7* processor running at 3.4 GHz. All algorithms were implemented using *MATLAB* software. For each case, a population of 10 individuals was used, represented as  $N_{ind} = 10$ , along with a maximum iteration count set to 50, denoted as  $It_{max} = 50$ .

After the simulation of the proposed mixed method, the solution of Case 1, and the best individual of each other cases can be found in Table 1.

Table 1. The solution of Case 1, and the best individual of each other cases

$X^*$	Case 1	Case 2	Case 3	Case 4	$X^*$	Case 1	Case 2	Case 3	Case 4
$K_{p,1}$	-1.2724	-1.2939	-0.9873	-1.2445	$R_{T,2}$	62.1442	58.1229	46.6081	53.6609
$R_{R,1}$	61.9467	59.5963	47.1668	57.2246	$T_{R,2}$	7.9239	8.0287	7.7383	7.9488
$T_{R,1}$	6.5530	6.1678	6.3945	6.0184	$K_{i,2}$	0.0363	0.0338	0.0392	0.0342
$K_{i,1}$	0.0596	0.0554	0.0746	0.0554	$K_{d,2}$	2.9469	2.7714	2.2134	3.0221
$K_{d,1}$	2.8898	2.8258	3.6123	2.5403	$T_{d,2}$	0.5748	0.5341	0.4324	0.5656
$T_{d,1}$	0.5749	0.5919	0.4819	0.5284	$B_1$	0.9532	0.9426	0.8984	0.9971
$K_{i,v}$	0.9247	0.8928	0.6973	0.8932	$B_2$	0.8155	0.7955	0.8532	0.8203
$K_{dc,v}$	2.4376	2.4662	1.8500	2.0187	$g_1$	0.2591	0.2711	0.2599	0.1662
$K_{p,2}$	-0.7992	-0.7401	-0.6560	-0.7378	$g_2$	0.2571	0.2553	0.2754	0.2511

Table 2 displays the fitness value for each case. It should be emphasized that Case 1 has the highest fitness value, indicating the effectiveness of the proposed hybrid model in searching for a better solution. Although the proposed approach spend more time consumption when compared with interior point method(case-1), the solution of this class of the problem is performed in off line. In other word, computational time is not a priority.

Table 2. Fitness function and simulation time values for each case

Case	1	2	3	4
Fitness	1430.2125	90.9981	82.1811	64.1351
Time (sec.)	1235.38	1167.09	1367.61	1337.21

Considering the solution obtained by using the proposed method, the results are displayed only for cases 1 and 4 because the solution of cases 2 and 3 are too close to case-4 . In this way, Figures 3(a) and 3(b) illustrate the frequency deviations of areas 1 and 2, respectively. It should be noted the improvement obtained with the use of the proposed approach (case-4), where the frequency deviation presents less oscillations. Although the VSG is installed in Area-1, some improvement has been found at Area-2 as well. On the other hand, the adjustable control reached by the proposed methodology is suitable to improve all connected power system.

Figures 4(a) and 4(a) displays the deviation in active power generation of the hydro plants for areas 1 and 2, respectively. It can be observed that the generation of the hydraulic power plants increases progressively until it matches the entire load variation in a steady state. This phenomenon stems from the swift action of the Virtual Synchronous Generator (VSG), which effectively absorbs a significant portion of the load variation in the initial moments after the disturbance. This action serves to prevent substantial inverse responses in the hydraulic turbines and abrupt fluctuations in generation. Subsequently, the load gradually shifts to the hydraulic plants due to the influence of the wind generation dispatch control. This control mechanism restores the VSG generation variation to zero in steady state. The insights gleaned from this analysis are further validated by Figure 5(a), which depicts the generation variation of the VSG. These characteristics are more evident in case-4 where the variables were optimized via proposed mixed algorithm.

Figure 5(b) shows the tie-line power deviation. Once again, the improvement obtained with the adjustment of the variables through the proposed methodology can be confirmed. That is, the reduction in oscillations as well as the time to reach steady state were greatly reduced.

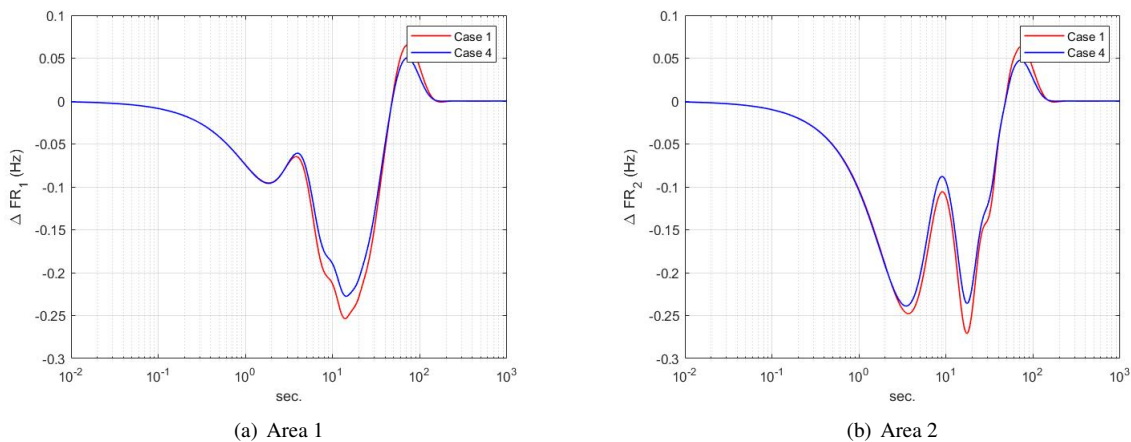


Figure 3. Frequency deviations

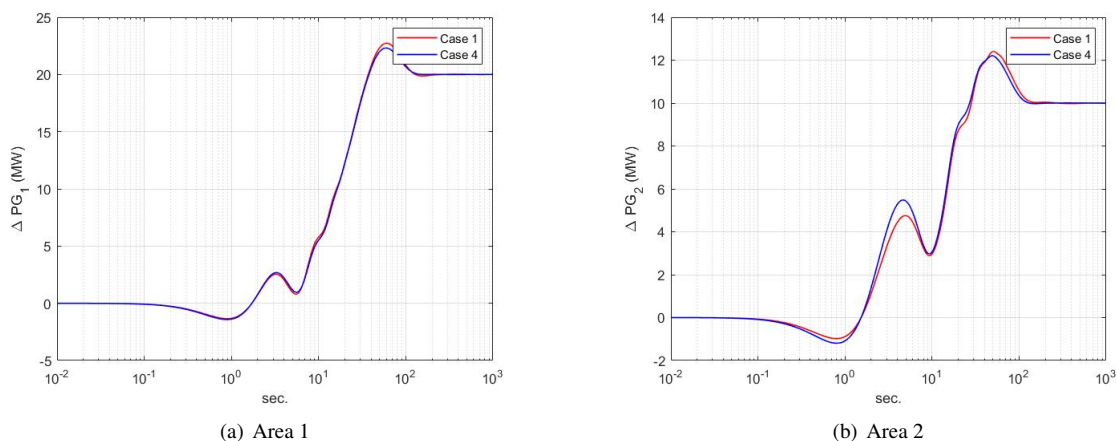


Figure 4. Hydro power generation deviations

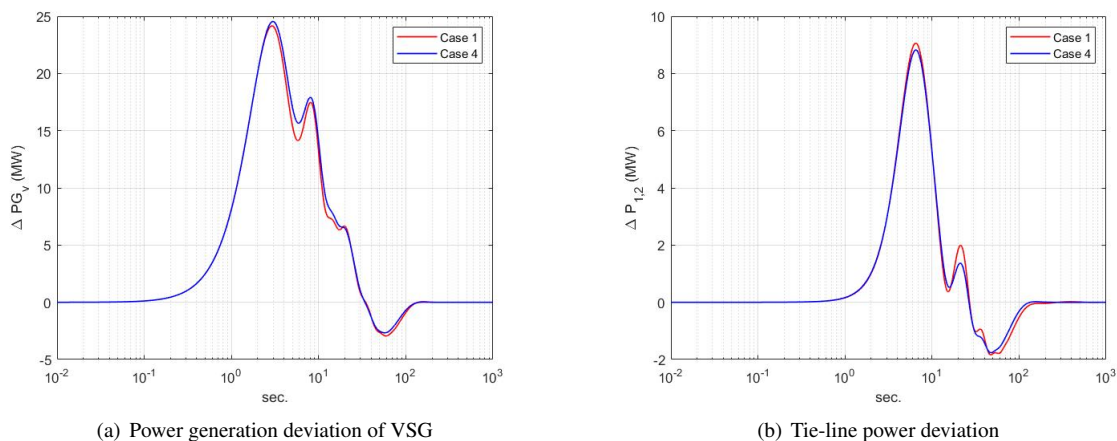


Figure 5. Power deviations of VSG and Tie-line

## 4 Conclusions

This paper presented a novel methodology for tuning Load Frequency Control (LFC) parameters in a hydro-wind interconnected power system. This approach combines nonlinear programming with the Manta Ray Foraging Optimization (MRFO) metaheuristic. The results demonstrate the promising nature of this methodology, highlighting the following key aspects:

- The proposed hybrid methodology achieves notable reductions in both frequency deviations and system interchange power flow.
- The fitness values attained through simulations employing the proposed hybrid methodology are consistently smaller than those obtained using the interior point method.
- The VSG prevents extensive power variations in the hydro turbines, resulting in reduced frequency deviations mainly for optimized control using the mixed approach.

For future studies and research, the inclusion of wind variability in the model and the exploration of secondary frequency control within the Generator Speed Variation (GSV) control scheme should be considered.

**Acknowledgements.** The authors acknowledge CAPES, CNPq, FAPEMIG and INERGE for their support.

**Authorship statement.** The authors hereby confirm that they are the sole liable persons responsible for the authorship of this work, and that all material that has been herein included as part of the present paper is either the property (and authorship) of the authors, or has the permission of the owners to be included here.

## References

- [1] IEA. *Renewables Data Explorer*. International Energy Agency, 2022.
- [2] ONS. Histórico da operação - capacidade instalada. *Operador Nacional do Sistema*, 2023.
- [3] da G. S. Silva, de E. J. Oliveira, de L. W. Oliveira, de A. N. Paula, J. S. Ferreira, and L. M. Honório. Load frequency control and tie-line damping via virtual synchronous generator. *International Journal of Electrical Power & Energy Systems*, vol. 132, pp. 107108, 2021.
- [4] P. S. Kundur and O. P. Malik. *Power system stability and control*. McGraw-Hill Education, 2022.
- [5] W. G. P. Mover and E. Supply. Hydraulic turbine and turbine control models for system dynamic studies. *IEEE Transactions on Power Systems*, vol. 7, n. 1, pp. 167–179, 1992.
- [6] M. D. Center. Optimization toolbox, constrained optimization, fmincon, 2020.
- [7] W. Zhao, Z. Zhang, and L. Wang. Manta ray foraging optimization: An effective bio-inspired optimizer for engineering applications. *Engineering Applications of Artificial Intelligence*, vol. 87, pp. 103300, 2020.
- [8] A. Mohammed, I. H. Hassan, M. D. Abdullahi, I. Aliyu, and J. Kim. Manta ray foraging optimization algorithm: Modifications and applications. *IEEE Access*, 2023.
- [9] X.-Y. Zhang, W.-K. Hao, J.-S. Wang, J.-H. Zhu, X.-R. Zhao, and Y. Zheng. Manta ray foraging optimization algorithm with mathematical spiral foraging strategies for solving economic load dispatching problems in power systems. *Alexandria Engineering Journal*, vol. 70, pp. 613–640, 2023.
- [10] S. Li, X. Kong, L. Yue, C. Liu, M. A. Khan, Z. Yang, and H. Zhang. Short-term electrical load forecasting using hybrid model of manta ray foraging optimization and support vector regression. *Journal of Cleaner Production*, vol. 388, pp. 135856, 2023.
- [11] M. A. Sobhy, H. M. Hasanien, A. Y. Abdelaziz, and M. Ezzat. Manta ray foraging optimization algorithm-based load frequency control for hybrid modern power systems. *IET Renewable Power Generation*, vol. 17, n. 6, pp. 1466–1487, 2023.
- [12] Z. Yuan, M. Xu, Y. Tao, M. Li, Z. Guo, and J. Zhang. Calculation of renewable energy hosting capacity of distribution network based on multi strategy improved adaptive manta ray foraging optimization. *Frontiers in Energy Research*, vol. 10, pp. 985623, 2023.
- [13] H. Shabani, B. Vahidi, and M. Ebrahimpour. A robust pid controller based on imperialist competitive algorithm for load-frequency control of power systems. *ISA transactions*, vol. 52, n. 1, pp. 88–95, 2013.